Chapter 7

Plasma instabilities

Stability and the loss of it, the instability, are central concepts in plasma physics. We have already dealt with many issues related to plasma stability, e.g., the change of magnetic connectivity in MHD is an instability, excitation of a wave mode in a plasma tells that the plasma is unstable to that mode, etc. Similarly to the large number of wave modes there is a rich flora of plasma instabilities. Actually, the topic is even wider than the family of linear wave modes, because a growing instability may develop to a nonlinear regime and cannot any more be described in terms of small wave-like perturbations. MHD shocks are examples of this feature.

7.1 Concept of instability

The basic idea of stability can be illustrated by a mechanical analogue of a ball which may be in a valley, on the top of a hill, on a plateau, or in a localized "crater" of a mountain. The physical system consists of both the ball and the landscape. The ball can represent the plasma particles and the landscape the fields confining the plasma, or something more abstract.

If the ball is in so deep valley that no realistic perturbation can lift it away from the valley, the system is **stable**. After the initial perturbation the ball returns back to its equilibrium position. It may oscillate around the bottom of the valley for a long time if the damping of the oscillation is slow.

If the ball is at the summit of the mountain, any perturbation moves it away from the hill and the system is **unstable**. After the perturbation the system finds a new equilibrium which may be completely different from the original. One may ask, how the ball did get to the unstable position in the first place. The answer is that the physical system includes both the ball and the landscape and in a time-dependent system the mountain may itself evolve with the time.

An example of an unstable system is the Harris current sheet discussed in Chapter 2. The current sheet evolves responding to the changing magnetic field configuration. As the field approaches the one-dimensional configuration, the current sheet becomes unstable to any perturbation and the system finally collapses to a lower state of energy.

A ball on a plateau represents a **meta-stable** state. The perturbation puts the ball in motion but the system looks the same until the ball reaches either an uphill or downhill region. For example, the solar wind-magnetosphere system is never in stable equilibrium but may look the same for a long period. Sooner or later the system develops to a state where its stability properties change.

Finally, the stability often depends on the strength of the perturbation. A ball in a crater remains there unless the perturbation is strong enough to pull the ball from the crater and let it roll down the hill. This case can, somewhat inaccurately, be called a **nonlinear instability**.

Our ability for a rigorous analysis of plasma stability is often limited to the linear regime, i.e., we can determine whether plasma is stable or unstable to small perturbations. If plasma is stable, the perturbation is damped. For a small damping rate ($|\omega_i| \ll \omega_r$) the perturbation is a normal mode of the plasma but often the damping takes place very quickly and the mode is overdamped. If $\omega_i > 0$, the wave grows and we have an instability. Without doing actual calculations it is usually impossible to say to how large amplitude a wave can grow. If nothing quenches the growth, the system develops to a major configurational change. However, often the growth leads to a situation where some plasma particles start to interact more strongly with the growing wave, e.g., by heating. This can sometimes be described in terms of the so-called **quasi-linear saturation** within the Vlasov theory.

A way of categorizing plasma instabilities is to divide them between microscopic (kinetic) and macroscopic (configurational) instabilities. The division is the same as within plasma theory in general. A **macroinstability** is something that can be described by macroscopic equations in the configuration space. A **microinstability** takes place in the ($\mathbf{r}$,$\mathbf{v}$)-space and depends on the actual shape of the distribution function.

Although it sometimes looks as if the plasma would become unstable quite spontaneously, it is not quite true. The instabilities do not arise without **free energy**. The free energy may come from the magnetic configuration (e.g., the Harris current sheet), anisotropic plasma pressure, streaming of plasma particles with respect to each other, etc. Identification of the free energy source is essential to understand a given instability because different free energy sources may lead to very different consequences.

7.1.1 Beam-plasma modes

The simplest electrostatic dispersion equation leading to instability can be constructed by considering ions as a non-moving background, an electron background population (density n_0, $V_0 = 0$), and a cold electron beam (n_b, $\mathbf{V}_b$) streaming through the background. It is an easy exercise to derive the dispersion equation

$$\epsilon(\omega, \mathbf{k}) = 1 - \frac{\omega_{p0}^2}{\omega^2} - \frac{\omega_{pb}^2}{(\omega - \mathbf{k}\cdot\mathbf{V}_b)^2} = 0\,. \tag{7.1}$$

This equation describes the Langmuir oscillations of both the background electrons and the beam electrons, Doppler-shifted by the streaming velocity.

If we neglect the background plasma entirely ($\omega_{p0}^2 = 0$), the solutions of the dispersion equation are

$$\omega = \mathbf{k}\cdot\mathbf{V}_b \pm \omega_{pb}\,. \tag{7.2}$$

These solutions are called **beam modes**.

In stability problems consideration of energy is often essential. The energy density of an electromagnetic wave in a plasma is given by

$$W_w = \epsilon_0 \delta\mathbf{E}^* \cdot \epsilon \cdot \delta\mathbf{E} + \frac{|\delta\mathbf{B}|^2}{2\mu_0}\,, \tag{7.3}$$

where $\delta\mathbf{E}, \delta\mathbf{B}$ indicate the wave electric and magnetic fields. Here the magnetic permeability of the plasma is assumed to be $\mu = \mu_0$, which is usually a good approximation and thus the determination of magnetic energy is straightforward. The electric energy is more complicated because it depends on the dielectric properties of the plasma. After some calculation the electric field energy in the $(\omega, \mathbf{k})$-space (i.e., the spectral energy density) can be expressed by

$$W_w(\omega, \mathbf{k}) = \frac{\epsilon_0}{2} \left\langle |\delta\mathbf{E}(\omega, \mathbf{k})|^2 \right\rangle \frac{\partial[\omega\epsilon(\omega, \mathbf{k})]}{\partial\omega}\,. \tag{7.4}$$

Because the energy density and also the spectral energy density are real quantities the above expression contains the real part of $\epsilon(\omega, \mathbf{k})$ only. This formula for W_w expresses both the energy density of the electric field $W_E = \epsilon_0 |\delta E|^2/2$ and the energy in the wave motion of the particles to provide the polarization, i.e., the energy that can formally be considered to set up a displacement field $\mathbf{D}$.

Coming back to the beam-plasma mode, the ratio of the total wave energy and the electric field energy is

$$\frac{W_w}{W_E} = \frac{\partial[\omega\epsilon(\omega, \mathbf{k})]}{\partial\omega} = \omega\,\frac{\partial\epsilon(\omega, \mathbf{k})}{\partial\omega} = \frac{2\omega_{p0}^2}{\omega^2} + \frac{2\omega\omega_{pb}^2}{(\omega - \mathbf{k}\cdot\mathbf{V}_b)^3}\,. \tag{7.5}$$

The first part comes from the Langmuir waves and the second is the contribution of the beam mode. If the Doppler-shifted frequency of the beam mode is negative, its energy is **negative**. When the beam moves through the plasma, it must slow down by the electromagnetic interaction with the background. Then the negative energy mode loses energy, i.e., its negative amplitude grows! Thus the beam-plasma system can be unstable, depending on the actual plasma parameters.

7.1.2 Two-stream instability

The instability of the beam-plasma system is called the **two-stream instability**. Figure 7.1 illustrates the coupling between the Langmuir mode and the beam modes in the (ω, k)-space.

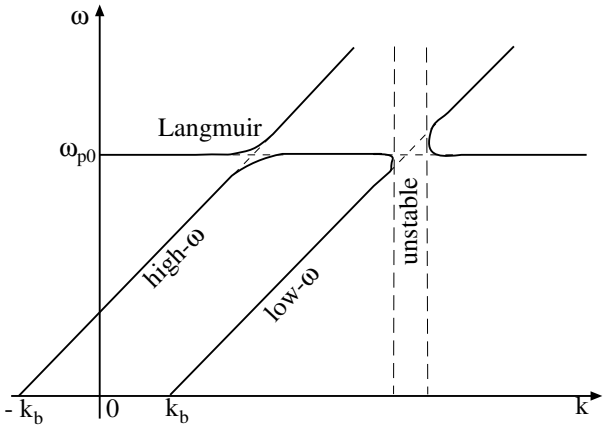

Figure 7.1: Coupling of Langmuir and beam-plasma modes

The solutions of the dispersion equation

$$1 - \frac{\omega_{p0}^2}{\omega^2} = -\frac{\omega_{pb}^2}{(\omega - \mathbf{k}\cdot\mathbf{V}_b)^2} \tag{7.6}$$

can be illustrated graphically by plotting its both sides separately, i.e., the ϵ_l (plasma oscillation) and $1 - \epsilon_b$ (1 – beam modes) (Figure 7.2). This graph shows that there are two (stable) solutions in the real plane whereas the second pair of solutions is in the complex plane. One of these is the unstable solution associated to the negative energy mode.

The analytical solution for the unstable mode can be found assuming that close to the phase velocity of the beam ($\omega \approx \pm kV_b$) the beam term is much larger than one. Then

$$\omega_{p0}^2(\omega - kV_b)^2 + \omega_{pb}^2\omega^2 = 0 \tag{7.7}$$

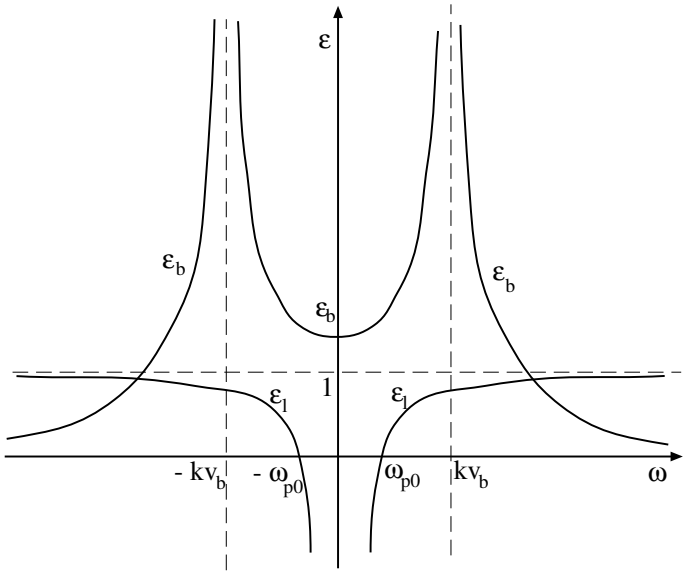

Figure 7.2: Graphical solution to illustrate the two-stream instability

$\Rightarrow$

$$\omega = \frac{kV_b}{2 + n_b/n_0} \left[1 \pm i \left(\frac{n_b}{n_0} \right)^{1/2} \right] . \tag{7.8}$$

Thus the negative energy mode of the two-stream instability has the frequency

$$\omega_{ts} = \frac{kV_b}{2 + n_b/n_0} \tag{7.9}$$

and the growth rate ($\gamma = \omega_i$)

$$\gamma = \omega_{ts} \left(\frac{n_b}{n} \right)^{1/2} . \tag{7.10}$$

The source of free energy is in the motion of the beam. If the beam is not continuously supported, the instability quenches itself after the beam has slowed down to a certain **threshold**. Ultimately the threshold is determined by the damping by the background particles, which is a microscopic process.

7.1.3 Buneman instability

A special type of two-stream instability arises when the entire electron population is streaming with respect to the ions in cold unmagnetized plasma. This is called the **Buneman instability**. It is an example of **current driven** instabilities because the relative motion of the particle populations yields a net current in the plasma. If the electrons and/or ions are so warm,

that their distribution functions overlap, microscopic treatment becomes necessary.

It is easiest to study the problem in the frame of the ions. Then the cold plasma dispersion equation is

$$\epsilon(\omega, \mathbf{k}) = 1 - \frac{\omega_{pi}^2}{\omega^2} - \frac{\omega_{pe}^2}{(\omega - kV_0)^2} = 0\,, \tag{7.11}$$

where V_0 is the relative velocity between the populations. Because $\omega_{pe} \gg \omega_{pi}$, the electron term dominates and the instability will appear for the slow negative energy mode $\omega_n \approx kV_0 - \omega_{pe}$, whereas the positive energy mode $\omega_p \approx kV_0 + \omega_{pe}$ is stable. Thus we can write

$$(\omega - \omega_n)\omega^2 = \frac{\omega_{pi}^2(\omega - kV_0)^2}{\omega - \omega_p}\,. \tag{7.12}$$

As in the two-stream case the interesting wave number is $k \approx \omega_{pe}/V_0$. Note, however, that now $\omega \ll \omega_{pe}$. With these approximations

$$\omega^3 \approx -\frac{m_e}{2m_i}\omega_{pe}^3\,. \tag{7.13}$$

This has one real root

$$\omega = -\left(\frac{m_e}{2m_i}\right)^{1/3}\omega_{pe}\,. \tag{7.14}$$

Writing $\omega \to \omega + i\gamma$ we obtain two equations

$$\omega(\omega^2 - 3\gamma^2) = -\frac{m_e\omega_{pe}^3}{2m_i} \tag{7.15}$$

$$\gamma^2 = 3\omega^2\,. \tag{7.16}$$

From these we find the maximally unstable Buneman mode

$$\omega_{bun} = \left(\frac{m_e}{16m_i}\right)^{1/3}\omega_{pe} \approx 0.03\omega_{pe} \tag{7.17}$$

$$\gamma_{bun} = \sqrt{3}\left(\frac{m_e}{16m_i}\right)^{1/3}\omega_{pe} \approx 0.05\omega_{pe}\,. \tag{7.18}$$

The growth rate of the mode is of the same order as its frequency. Thus the amplitude grows rapidly and can lead to rapid change of the configuration, e.g., transforming the free energy (current) to heat of the plasma. This is an example of **anomalous resistivity** where the instability takes the role of collisions to resist the current flow.

It is a good exercise to show that the unstable wave modes must have

$$k^2 V_0^2 < \omega_{pe}^2 \left[1 + \left(\frac{m_e}{m_i} \right)^{1/3} \right]^3 . \tag{7.19}$$

Thus the unstable wave must have a minimum wavelength. The frequency has its maximum (ω_{bun}) at this threshold and decreases toward longer waves. The instability quenches itself through a nonlinear process where the growing electric field fluctuations begin to trap electrons, slowing them down to a velocity which is below the threshold for the wave growth.

7.2 Macroinstabilities

Division between macro- and microinstabilities is mainly a technical matter. There are instabilities which can be treated in macroscopic theory although velocity space effects may be important in some stage of the evolution of the instability, in particular in saturation. In this section we discuss some of the most important macroscopic instabilities in space plasmas.

7.2.1 Rayleigh-Taylor instability

The Rayleigh-Taylor (R-T) instability is perhaps the simplest example of macroscopic instabilities arising from plasma inhomogeneities. Consider a heavy plasma supported against the gravitational force by magnetic field. Let the boundary between the heavy and light plasmas as well as the magnetic field be in the (x, y)-plane, $\mathbf{B}_0 = B_0 \mathbf{e}_x$, and let the gravitational acceleration $\mathbf{g} = -g\,\mathbf{e}_z$ act downward and the density gradient $\nabla n_0 = [\partial n_0(z)/\partial z]\mathbf{e}_z$ point upward. This kind of configurations appear, e.g., the equatorial ionosphere or in the solar atmosphere. Let the plasma be, for simplicity, collisionless and cold.

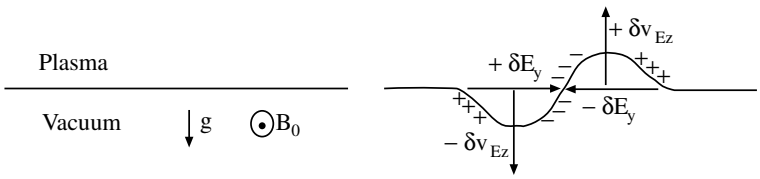

Figure 7.3: Principle of the Rayleigh-Taylor instability. The forming bubbles become unstable against the same instability and form smaller structures and gradually disappear.

Consider a small sinusoidal perturbation to the boundary. The gravitational field causes the ion drift and current in the $-y$-direction. This leads to

an electric field perturbation that is in the $+y$-direction in the region where there is plasma below the original boundary and in the opposite direction in the region where the perturbation has lifted the plasma boundary upward. Now, in the downward perturbed region the E×B-drift is downward and in the upward perturbed region upward. Thus the E×B-drift enhances the original perturbation and the system is unstable. The result is that the gravitationally supported plasma falls down and dilute bubbles rise up.

The dispersion equation for the R-T instability can be found starting from the cold ion equation of motion including the gravitational force. Assuming harmonic behavior of the ion velocity and the electric field perturbations we find

$$\left(\omega + \frac{gk_\perp}{\omega_{ci}}\right)\delta\mathbf{V}_{i\perp} = \frac{e}{m_i}(\mathbf{k}_\perp\delta\varphi - iB_0\mathbf{e}_x \times \delta\mathbf{V}_{i\perp})\,. \tag{7.20}$$

Because the frequency of the disturbance must be much smaller than ω_{ci} (why?) the solution for the velocity disturbance is

$$\delta\mathbf{V}_{i\perp} = -\delta\varphi\left[i\mathbf{k}_\perp \times \mathbf{e}_x + \frac{\mathbf{k}_\perp}{\omega_{ci}B_0}\left(\omega + \frac{gk_\perp}{\omega_{ci}}\right)\right]. \tag{7.21}$$

The ion continuity equation is now

$$\omega\delta n_i = n_0\mathbf{k}\cdot\delta\mathbf{V}_i - i\delta\mathbf{V}_i\cdot\nabla n_0 \tag{7.22}$$

Eliminating $\delta\mathbf{V}_i$ we get the density disturbance

$$\delta n_i = n_0\delta\varphi\left[\frac{e}{m_i}\left(\frac{k_\parallel^2}{\omega^2} - \frac{k_\perp^2}{\omega_{ci}^2}\right) + \frac{k_\perp}{B_0L_n}\left(\omega + \frac{gk_\perp}{\omega_{ci}}\right)^{-1}\right], \tag{7.23}$$

where L_n is the undisturbed density scale length

$$L_n^{-1} = \frac{d\ln n_0(z)}{dz} > 0\,. \tag{7.24}$$

Assuming that the electrons are cold and do not drift (the gravitational drift of electrons is a factor of m_e/m_i smaller than the ion drift), we get from the electron continuity and momentum equations the relation

$$\delta n_e = -\delta\varphi\frac{n_0}{B_0}\left(\frac{\omega_{ce}}{\omega}\frac{k_\parallel^2}{\omega} - \frac{k_\perp}{L_n\omega}\right). \tag{7.25}$$

Because the frequency is very small, the charge neutrality $\delta n_e = \delta n_i$ is maintained. Eliminating the fluctuating potential we find

$$\frac{\omega_{ci}}{\omega}\frac{1}{k_\perp L_n}\left(1 - \frac{\omega}{\omega + gk_\perp/\omega_{ci}}\right) - \left(1 + \frac{m_i}{m_e}\right)\frac{\omega_{ci}^2}{\omega^2}\frac{k_\parallel^2}{k_\perp^2} + 1 = 0\,. \tag{7.26}$$

To find exact solutions to this equation is a little tedious. The highest growth rate is found for exactly perpendicular propagation ($k_\parallel = 0$) because then the electric field will lead to the largest vertical drift. Assuming further a weak gravitational effect ($\omega \gg k_\perp g/\omega_{ci}$) the first order solution is

$$\omega^2 = -\frac{g}{L_n}\,, \tag{7.27}$$

which has a pure growing solution with the growth rate

$$\gamma_{0rt} = \left(\frac{g}{L_n}\right)^{1/2} \tag{7.28}$$

This is the same growth rate as in the non-magnetic fluid case.

Expanding the dispersion equation to the second order in $k_\perp g/(\omega_{ci}\omega)$ we could find an oscillating solution but still the growth rate is much larger than the oscillation frequency. Letting $k_\parallel \neq 0$, solutions would still be found limited in a very narrow cone around the perpendicular direction.

The gravitational acceleration decreases with increasing distance as r^{-2}. At the Earth this implies that the R-T instability is important only in the ionosphere, and because the magnetic field must be horizontal, only in the equatorial ionosphere. In fact, radar and satellite observations have verified the existence of rising low-density bubbles from the F-region above 200 km. This effect is called **equatorial spread-F**. Bubbles can rise up to about 1000 km altitude with upward velocities of about 100 m/s.

Neither the ionosphere nor the partially ionized parts of the solar atmosphere are fully collisionless. Electrons can still be taken as collision-free but the ion-neutral collision rate ν_{in} as well as the pressure force must be taken into account. The analysis becomes slightly more complicated than in the collisionless case. The collisional growth rate is found to be

$$\gamma_{rt} = \gamma_{0rt}\left[1 - \exp\left(-\frac{\gamma_{0rt}}{\nu_{in}}\right)\right]\,, \tag{7.29}$$

which at the limit of vanishing collisions yields γ_{0rt}. At the limit of large collision frequency the growth rate becomes

$$\gamma_{rtn} = \frac{g}{\nu_{in}L_n} = \frac{\gamma_{0rt}^2}{\nu_{in}}\,. \tag{7.30}$$

Note that in astrophysics the Rayleigh-Taylor instability is often called **Kruskal-Schwarzschild instability**-

7.2.2 Farley-Buneman instability

The Farley-Buneman (F-B) instability is related to the R-T instability. It is also driven by the horizontal currents, but now the currents are not of gravitational character and the magnetic field does not need to be horizontal.

The basic physics is easiest to calculate for the equatorial case where the magnetic field is horizontal and the electric field points vertically downward: $\mathbf{E}_0 = -E_0\,\mathbf{e}_z$. Consequently the drift is eastward $V_E = -E_0/B_0$. The linearized electron continuity equation can be written as

$$\delta V_{ey} = \left(\frac{\omega}{k_\perp} - V_E\right)\frac{\delta n}{n_0}\,, \tag{7.31}$$

where quasi-neutrality is assumed. Neglecting the electron inertia and the gravitation but retaining the electron-neutral collisions, the linearized electron momentum equation has two components

$$\omega_{ce}\delta V_{ey} + \nu_{en}\delta V_{ez} = 0 \tag{7.32}$$

$$\nu_{en}\delta V_{ey} - \omega_{ce}\delta V_{ez} = -ik_\perp\left(\frac{e}{m_e}\delta\varphi - \frac{k_B T_e}{m_e}\frac{\delta n}{n_0}\right). \tag{7.33}$$

Due to high ν_{in} the ions do not move in the vertical direction and thus the ion continuity and momentum equations are

$$\delta V_{iy} - \frac{\omega}{k_\perp}\frac{\delta n}{n_0} = 0 \tag{7.34}$$

$$(\omega - i\nu_{in})\delta V_{iy} - k_\perp v_{thi}^2\frac{\delta n}{n_0} = \frac{e}{m_i}k_\perp\delta\varphi\,. \tag{7.35}$$

This set of linear equations has nontrivial solutions when the coefficient matrix has a zero determinant. This gives us the dispersion equation

$$\omega\left(1 + i\psi_0\frac{\omega - i\nu_{in}}{\nu_{in}}\right) = k_\perp V_E + i\psi_0\frac{k_\perp^2 c_s^2}{\nu_{in}}\,, \tag{7.36}$$

where

$$\psi_0 = \frac{\nu_{en}\nu_{in}}{\omega_{ce}\omega_{ci}}$$

and the ion-acoustic speed is defined by $c_s^2 = k_B(T_e + T_i)/m_i$.

For a weakly unstable solution we find the frequency

$$\omega_{fb} = \frac{k_\perp V_E}{1 + \psi_0} \tag{7.37}$$

and the growth rate

$$\gamma_{fb} = \frac{\psi_0}{\nu_{in}}\frac{\omega_{fb}^2 - k_\perp^2 c_s^2}{1 + \psi_0}\,. \tag{7.38}$$

Thus the F-B instability sets in when the wave phase speed exceeds the ion acoustic speed, or equivalently, when the drift speed exceeds the threshold

$$V_E > (1 + \psi_0)c_s \,. \tag{7.39}$$

The collision frequencies depend on the neutral density that follows the barometric law $n_n(z) \propto \exp(-z/H)$. In the equatorial ionosphere $\psi_0 \approx 0.22$ at the altitude of 105 km and decreases rapidly upward, making the growth rate negligible above altitudes of 130–150 km. Thus the F-B instability is limited to the E-region ionosphere.

The F-B instability is observed also in the auroral ionosphere where the geometry is different and there are other mechanisms to make the observed spectra more complicated. The F-B fluctuations are used in ionospheric diagnostics of the auroral ionosphere because they coherently scatter electromagnetic waves (Chapter 9). A coherent ionospheric radar sends waves of a few meter wavelength and detects the backscattered signal. The scattering occurs when the wave front crosses the background magnetic field at right angles. From the Doppler shift of the backscattered signal it is possible to derive the component of the drift speed in the direction of the wave. Using two such radars at different locations it is possible to determine the electric field assuming that it is perpendicular to the background magnetic field which is a good assumption in the ionosphere.

7.2.3 Kelvin-Helmholtz instability

The Kelvin-Helmholtz (K-H) instability is basically a neutral fluid phenomenon illustrated by the wind blowing over water and causing ripples on the surface. The same happens in collisional and collisionless plasmas, e.g., the solar wind flow along the magnetopause causes the K-H instability and the K-H waves propagate on the bounding surface.

As an example we study the instability on the magnetopause in the ideal MHD scale. At the narrow boundary there may be some viscous effects (e.g., anomalous viscosity through wave-particle interactions) but they are higher order corrections to this discussion. Let the magnetic field and the flow be tangential to the boundary and let the velocity change, or reverse, across the boundary. Assume scalar pressure, linearize around background $\mathbf{B}_0$ and n_0, and consider small displacements $\delta\mathbf{x}$ defined by $\delta\mathbf{V} = d\delta\mathbf{x}/dt$. The strategy is to linearize the induction and momentum equations and find an expression for $\delta\mathbf{x}$. The linearized equations are

$$\begin{aligned} \delta\mathbf{B} &= \nabla \times (\delta\mathbf{x} \times \mathbf{B}_0) \qquad (7.40)\\ &= \mathbf{B}_0 \cdot \nabla\delta\mathbf{x} - \delta\mathbf{x} \cdot \nabla\mathbf{B}_0 - \mathbf{B}_0\nabla \cdot \delta\mathbf{x} \\ \mu_0 m_i n_0 d^2\delta\mathbf{x}/dt^2 &= -\mu_0\nabla\delta p + \qquad (7.41)\\ &\quad -\delta\mathbf{B} \times (\nabla \times \mathbf{B}_0) - \mathbf{B}_0 \times (\nabla \times \delta\mathbf{B}) \,, \end{aligned}$$

where the induction equation has been integrated with respect to t. Define the first order variation in the the total pressure as

$$\mu_0 \delta p_{tot} = \mu_0 \delta p + \mathbf{B}_0 \cdot \delta \mathbf{B} \,. \tag{7.42}$$

Eliminating the magnetic field perturbation we get

$$m_i n_0 \left[(\mathbf{v}_A \cdot \nabla)^2 - \frac{\partial^2}{\partial t^2} \right] \delta \mathbf{x} = \nabla \delta p_{tot} + \mathbf{C} \,. \tag{7.43}$$

The Alfvén velocity is defined for the background parameters and the vector $\mathbf{C}$ contains the remaining terms. This equation shows that the Alfvén wave is coupled to the pressure fluctuations. Because the divergence of the background magnetic field and the magnetic field variations must vanish, equations (7.40–41) yield another equation for the total pressure variation

$$\nabla^2 \delta p_{tot} = -m_i \nabla \cdot \left(n_0 \frac{d^2 \delta \mathbf{x}}{dt^2} \right) + \frac{1}{\mu_0} \nabla \times (\delta \mathbf{B} \cdot \nabla \mathbf{B}_0 + \mathbf{B}_0 \cdot \nabla \delta \mathbf{B}) \,. \tag{7.44}$$

Assume now that the the plasma and the flow are homogeneous on both sides of the boundary. This implies that the plasma is incompressible ($\nabla \cdot \delta \mathbf{V} = 0$). With this assumption the RHS of equation (7.44) vanishes as does $\mathbf{C}$:

$$\nabla^2 \delta p_{tot} = 0 \,. \tag{7.45}$$

The only change in δp_{tot} occurs at the thin boundary and the pressure disturbance fades out with increasing distance from the boundary.

Let the boundary be in the (x, z)-plane and assume plane wave solutions for both $\delta \mathbf{x}$ and δp_{tot} with wave number $\mathbf{k} = k_x \mathbf{e}_x + k_z \mathbf{e}_z$ and frequency ω. Now we can solve the displacement of the boundary

$$\delta \mathbf{x} = \frac{\delta p_{tot}}{m_i n_0 [\omega^2 - (\mathbf{k} \cdot \mathbf{v}_A)^2]} \tag{7.46}$$

and the solution of the Laplace equation for δp_{tot} is

$$\delta p_{tot} = p_0 \exp(-k|y|) \exp[-i(\omega t - k_x x - k_z z)] \,, \tag{7.47}$$

where $k^2 = k_x^2 + k_z^2$. The y-dependence is selected to make the wave evanescent outside the boundary because there is free energy only at the boundary.

We consider the boundary as a tangential discontinuity, i.e., a boundary through which there is no plasma flow and $B_n = 0$ but V_t, B_t, n, and p may jump at the boundary. We further require that the normal component of the displacement is continuous. Denote the two sides of the boundary by 1 and 2 and let the plasma stream with velocity $\mathbf{V}_0$ in region 1 and let the fluid in region 2 be in rest. Because the total pressure $p + B^2/2\mu_0$

is continuous, the continuity of the normal component of the displacement yields the dispersion equation for the K-H waves

$$\frac{1}{n_{02}[\omega^2-(\mathbf{k}\cdot\mathbf{v}_{A2})^2]}+\frac{1}{n_{01}[(\omega-\mathbf{k}\cdot\mathbf{V}_0)^2-(\mathbf{k}\cdot\mathbf{v}_{A1})^2]}=0\,. \tag{7.48}$$

This equation is quite similar to the equations for streaming instabilities. Now the unstable modes are not plasma oscillations but Alfvén waves. The dispersion equation has an unstable solution

$$\omega_{kh}=\frac{n_{01}\mathbf{k}\cdot\mathbf{V}_0}{n_{01}+n_{02}} \tag{7.49}$$

corresponding to the complex root

$$(\mathbf{k}\cdot\mathbf{V}_0)^2>\frac{n_{01}+n_{02}}{n_{01}n_{02}}[n_{01}(\mathbf{k}\cdot\mathbf{V}_{A1})^2+n_{02}(\mathbf{k}\cdot\mathbf{V}_{A2})^2]\,. \tag{7.50}$$

The K-H instability occurs thus for sufficiently large $\mathbf{V}_0$. For small $\mathbf{V}_0$ k would have to be too large, i.e., the wavelength too short for the MHD description to be valid.

At the limit where the spatial scale becomes comparable to the ion gyroradius the finite gyroradius effects introduce kinetic properties to Alfvén waves. There are two types of **kinetic Alfvén** waves. For relatively large beta ($\beta > m_e/m_i$), e.g., at the magnetospheric boundary, the mode is called the **oblique kinetic Alfvén wave** with the phase velocity components

$$\begin{aligned} v_\parallel &= v_A\left[1+k_\perp^2 r_{Li}^2\left(\frac{3}{4}+\frac{T_e}{T_i}\right)\right]^{1/2} \\ v_\perp &= \frac{k_\parallel v_A}{k_\perp}\left[1+k_\perp^2 r_{Li}^2\left(\frac{3}{4}+\frac{T_e}{T_i}\right)\right]^{1/2}\,. \end{aligned} \tag{7.51}$$

Referring to the K-H unstable configuration, we can expect that the wavelength along the magnetic field (which is tangential to the bounding surface) is much longer than the perpendicular wavelength, i.e., $k_\parallel \ll k_\perp$.

The K-H instability is important also in the low-beta plasma, e.g., above the auroral arcs. From satellite and radar observations we know that above auroral arcs the electric field points toward the arc on both sides. Thus the plasma flow on both sides of the arc is in almost opposite direction. The K-H instability arising from the shear flow is a popular explanation of why auroral arcs develop to folds and spirals.

In the auroral region the kinetic effects are different. As now $\beta \ll m_e/m_i$, the electron thermal speed is smaller than the Alfvén speed ($v_{the} < v_A$), and

the electron inertia must be taken into account. The wave is called the **shear kinetic Alfvén wave** and its dispersion equation reads as

$$\omega^2 = k_\parallel^2 v_A^2 \frac{1 + k_\perp^2 r_{Li}^2}{1 + k_\perp^2 c^2/\omega_{pe}^2}\,, \tag{7.52}$$

where the ratio c/ω_{pe} is the so-called **electron inertial length**. Consequently some authors call the wave the **inertial kinetic Alfvén wave**.

The kinetic Alfvén waves are important in the magnetosphere-ionosphere coupling as the are able to carry the field-aligned current and set up small-scale parallel electric fields. As the Alfvén waves are electromagnetic waves we can express the wave electric field in terms of the vector potential only $\delta\mathbf{E} = -\partial\mathbf{A}/\partial t$ (this is the so-called temporal gauge introduced in Ch. 1. Assuming gyrotropy, we can reduce the vector potential and the electric field to two dimensions $(\perp, \parallel)$ and express the electric field in terms of two potential functions

$$\delta\mathbf{E} = -(\nabla_\perp\varphi_\perp, \nabla_\parallel\varphi_\parallel)\,. \tag{7.53}$$

Because there are no space charges, Poisson's equation yields

$$\nabla_\perp^2\varphi_\perp + \nabla_\parallel^2\varphi_\parallel = 0\,. \tag{7.54}$$

From the time derivative of the Ampère's law we can calculate

$$\begin{aligned}
\mu_0\frac{\partial\mathbf{J}}{\partial t} &= \nabla\times\left(\nabla\times\frac{\partial\mathbf{A}}{\partial t}\right)\\
&= \nabla\times(\nabla\times(\nabla_\perp\varphi_\perp, \nabla_\parallel\varphi_\parallel))\\
&= \nabla_\parallel\nabla_\perp^2(\varphi_\perp - \varphi_\parallel)\mathbf{b}\,,
\end{aligned} \tag{7.55}$$

i.e., the fluctuation in the wave electric field has a magnetic field-aligned component and this is related to the field-aligned component of the current.

7.2.4 Firehose instability

The firehose instability has an analogue in an ordinary fire- or garden hose with a rapid water flow. Small perturbation may cause a violent motion of the hose needing several firemen to hold it in the right direction. In ideal anisotropic MHD a magnetic flux-tube corresponds to the hose and the parallel pressure to the flowing water.

We can start the analysis from equation (3.58) of the CGL theory

$$\rho_m\left(\frac{d\mathbf{V}}{dt}\right)_\perp + \nabla_\perp\left(p_\perp + \frac{B^2}{2\mu_0}\right) - \frac{(\mathbf{B}\cdot\nabla)\mathbf{B}}{\mu_0}\left(\frac{p_\perp - p_\parallel}{B^2/\mu_0} + 1\right) = 0\,. \tag{7.56}$$

Assuming $\mathbf{V}_0 = 0$ and $\mathbf{B} = \mathbf{B}_0 + \mathbf{B}_1$, where $\mathbf{B}_1$ is a small perturbation, and linearizing, we get the dispersion equation

$$\begin{aligned} \omega^2 &= \frac{k^2}{2\rho_{m0}} \left\{ \left(\frac{B_0^2}{\mu_0} + p_\perp + 2p_\parallel \cos^2\theta + p_\perp \sin^2\theta \right) + \right. \\ &\pm \left. \sqrt{\left(\frac{B_0^2}{\mu_0} + p_\perp(1+\sin^2\theta) - 4p_\parallel \cos^2\theta \right)^2 + 4p_\perp^2 \sin^2\theta \cos^2\theta} \right\} . \end{aligned} \tag{7.57}$$

For perpendicular propagation ($\theta = \pi/2$) this reduces to

$$\frac{\omega^2}{k^2} = \frac{2}{\rho_{m0}} \left(\frac{B_0^2}{2\mu_0} + p_\perp \right) , \tag{7.58}$$

which is the stable magnetosonic mode with the phase velocity $\sqrt{v_A^2 + v_s^2}$. For parallel propagation there are two solutions. The sound wave

$$\omega^2 = \frac{3k^2}{\rho_{m0}} p_\parallel \tag{7.59}$$

and another mode with the dispersion equation

$$\omega^2 = \frac{k^2}{\rho_{m0}} \left(\frac{B_0^2}{\mu_0} + p_\perp - p_\parallel \right) . \tag{7.60}$$

At the isotropic limit the latter is the Alfvén wave ($\omega/k = v_A$). If $p_\parallel > p_\perp + B_0^2/\mu_0$, the wave has an unstable solution, the firehose instability. The dispersion equation can be written in terms of parallel and perpendicular beta and the threshold can be expressed as (exercise)

$$\beta_{0\parallel} > \beta_{0\perp} + 2 . \tag{7.61}$$

Due to the requirement $\beta > 2$ the firehose instability requires very low magnetic field or strong pressure, this is possible in the solar wind or in the magnetotail neutral sheet. Once excited the instability is strong.

7.2.5 Mirror instability

The mirror instability is complementary to the firehose instability and propagates nearly perpendicular to the magnetic field. Its dispersion equation is straightforward (but not easy) to derive from kinetic theory retaining contributions from all particle species. This procedure yields unstable solutions for both parallel and perpendicular directions. In the parallel direction the firehose threshold is found in the form

$$\sum_\alpha \beta_{\alpha\parallel} > 2 + \sum_\alpha \beta_{\alpha\perp} . \tag{7.62}$$

For perpendicular propagation the threshold for the mirror instability is

$$\sum_\alpha \frac{\beta_{\alpha\perp}^2}{\beta_{\alpha\|}} > 1 + \sum_\alpha \beta_{\alpha\perp} \,. \tag{7.63}$$

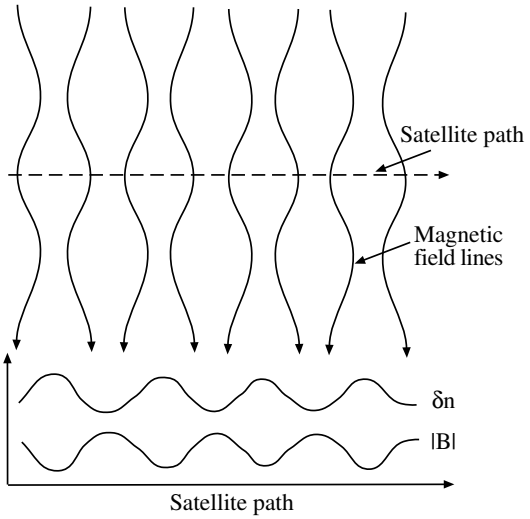

Figure 7.4: Sketch of satellite observations of plasma density and magnetic field fluctuations throug a mirror-unstable region

Figure 7.4 illustrates how a mirror unstable region looks in satellite data and why the mode is called the mirror mode: Part of the plasma is trapped in the small magnetic bottles of the wave. The mode has been observed in the dayside magnetosheath where the shocked solar wind plasma is adiabatically heated in the perpendicular direction but at the same time the field-aligned flow around the magnetopause lowers the parallel temperature, leading to favorable conditions for the mirror instability to develop.

7.2.6 Flux tube instabilities

Flux tube instabilities are particularly important in solar physics (as well as in laboratory devices). Their stability analysis is usually based on the energy principle. In the method the energy content of the system is calculated in presence of small perturbations. If the energy variation $\triangle W$ is negative, the system is unstable. The calculations are usually cumbersome.

There are three basic modes of instabilities in flux tubes carrying a longitudinal current. The magnetohydrostatic equilibrium ($\mathbf{J} \times \mathbf{B} = \nabla p$) is in all cases maintained by the azimuthal magnetic field (so called **linear pinch**).

In the **pinch instability** arises from squeezing (pinching) the flux tube. The azimuthal field is increased in regions where the tube is pinched and decreased outside. Thus the pinching self-amplifies the instability. This instability is important in certain laboratory settings and it may take place in the active regions of the solar corona. In the magnetosphere the background magnetic field is so strong that the pinch configuration cannot develop.

The **kink instability** resembles the pinch effect. If the tube is kinked, there is an inward pressure gradient in the inner edge of the kink and outward pressure gradient in the outer edge. Again the perturbation is self-amplifying, i.e., unstable. Also this process may be excited in the solar corona or in the magnetospheric tail current sheet.

Finally, the **helical instability** is probably common in the solar corona where strongly twisted flux tubes are frequently appear. This instability requires strong enough field-aligned current to flow through the structure. Solar prominences are examples of helical magnetic field structures.

7.3 Electrostatic instabilities

We start the discussion of microinstabilities from the electrostatic instabilities. The central element of microscopic theory is the dispersion equation and our task is now to find out when it has growing solutions.

7.3.1 Monotonically decreasing distribution function

Let $f_{\alpha 0}(\mathbf{v})$ decrease monotonically and consider electrostatic perturbation

$$f_\alpha = f_{\alpha 0} + f_{\alpha 1}(\mathbf{v}) \exp[i(\mathbf{k}\cdot\mathbf{r} - \omega t)]\,, \tag{7.64}$$

where ω is a solution of the dispersion equation

$$1 - \frac{\omega_{pe}^2}{k^2} \int\limits_{-\infty}^{\infty} \frac{1}{u - \omega/|k|} \frac{\partial}{\partial u} \left[F_{e0}(u) + \frac{m_e}{m_i} F_{i0}(u) \right] du = 0\,. \tag{7.65}$$

Here we have assumed two populations (electrons and ions) and $F_{\alpha 0}$ is the one-dimensional distribution function. If the dispersion equation implies that $\omega_i > 0$, the distribution function is unstable, otherwise it is stable.

Assume now that $\omega_i > 0$. Thus the pole of (7.65) is in the upper half plane and the integral can be taken along the real u-axis. Denote $F = F_{e0} + (m_e/m_i)F_{i0}$. Then the dispersion equation reduces to

$$1 \quad - \quad \frac{\omega_{pe}^2}{k^2} \int\limits_{-\infty}^{\infty} \frac{u - \omega_r/|k|}{(u - \omega_r/|k|)^2 + \omega_i^2/k^2} \frac{\partial F}{\partial u}\, du \tag{7.66}$$

$$- \quad \frac{i\omega_i}{|k|}\frac{\omega_{pe}^2}{k^2}\int\limits_{-\infty}^{\infty}\frac{\partial F/\partial u}{(u-\omega_r/|k|)^2+\omega_i^2/k^2}\,du = 0\,.$$

These integrals do not contain any singularities. Because the real and imaginary parts must both be zero, we have

$$\int\limits_{-\infty}^{\infty}\frac{\partial F/\partial u}{(u-\omega_r/|k|)^2+\omega_i^2/k^2}\,du = 0 \tag{7.67}$$

$$1-\frac{\omega_{pe}^2}{k^2}\int\limits_{-\infty}^{\infty}\frac{u(\partial F/\partial u)}{(u-\omega_r/|k|)^2+\omega_i^2/k^2}\,du = 0\,. \tag{7.68}$$

For a monotonically decreasing distribution $u(\partial F/\partial u) \leq 0$, i.e., the integral in (7.68) is negative definite and the equation has no solutions. Thus we have derived a contradiction from the assumption $\omega_i > 0$. This applies to all monotonic functions and the result is independent of the frame of reference. We cannot create an instability just by letting the observer to move with respect to the distribution.

7.3.2 Multiple-peaked distributions

Two-stream instability is produced by a multiple-peaked distribution. Consider the so-called gentle-bump distribution for the electrons

$$f_{e0} = \frac{n_1}{n_e}\left(\frac{m_e}{2\pi k_B T_1}\right)^{3/2}\exp\left(-\frac{m_e v^2}{2k_B T_1}\right)+\frac{n_2}{n_e}\delta(v_x)\delta(v_y)\left(\frac{m_e}{2\pi k_B T_2}\right)^{1/2}\times \frac{1}{2}\left\{\exp\left(-\frac{m_e(v_z-V_0)^2}{2k_B T_2}\right)+\exp\left(\frac{m_e(v_z+V_0)^2}{2k_B T_2}\right)\right\}. \tag{7.69}$$

where $n_e = n_1 + n_2 \gg n_2$, $T_2 \ll T_1$, $V_0 \gg 2k_B T_1/m_e$. We assume that the ions are cold $f_{i0} = \delta(v_x)\delta(v_y)\delta(v_z)$. Furthermore, in order to neglect the current driven by the bump we consider an electron distribution that is symmetric about $v_z = 0$ (thus the argument of f_{e0} in Fig. 7.5 is v_z^2).This way the problem remains strictly electrostatic.

In the absence of the bump the solution would be the damped Langmuir wave. Now the calculation of K_r and K_i is considerably more tedious than in the Maxwellian case. The procedure is, however, straightforward: Start with equations (6.40–41). Insert the distribution function (7.69) and consider long wavelengths. With the assumptions $n_1 \gg n_2$, $T_2 \ll T_1$ we find that the real part is that of the Langmuir wave

$$\omega_r = \omega_{pe}(1+3k^2\lambda_{De}^2)^{1/2} \approx \omega_{pe}(1+\frac{3}{2}k^2\lambda_{De}^2) \tag{7.70}$$

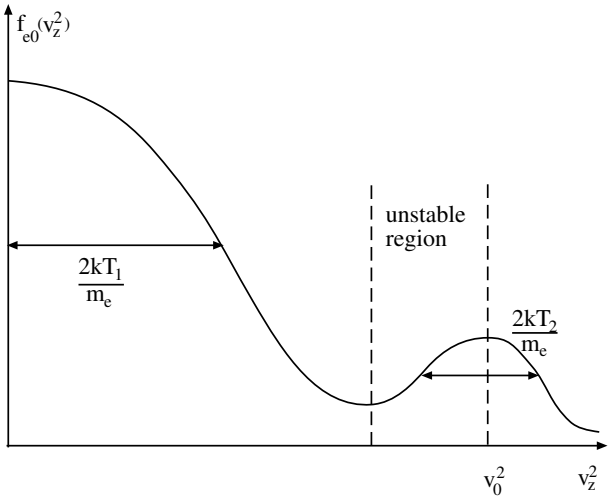

Figure 7.5: Gentle-bump distribution

The imaginary part is modified by a term depending on the relation between the bump and the background

$$\begin{aligned} \omega_i &= -\sqrt{\frac{\pi}{8}}\frac{\omega_{p1}}{|k^3\lambda_{D1}^3|}\exp\left(-\frac{1}{2k^2\lambda_{D1}^2}-\frac{3}{2}\right)+ \\ &+ \frac{n_2}{n_1}\left(\frac{T_1}{T_2}\right)^{3/2}\frac{k^3}{k_z^3}\left(\frac{k_zV_0}{\omega_r}-1\right)\exp\left\{-\frac{T_1/T_2}{2k^2\lambda_{D1}^2}\left(1-\frac{k_zV_0}{\omega_r}\right)^2\right\}. \end{aligned} \tag{7.71}$$

The first term is the Landau damping of the background. The second term is stabilizing to the right from the bump ($v_z > v_0$) where the distribution is decreasing but it **may** destabilize ($\omega_i > 0$) plasma oscillations to the left from the bump in between the two peaks of the distribution function. The essential point is whether or not the derivative of the full distribution function is positive $\partial f_{e0}/\partial v > 0$ and large enough somewhere. If it is, we have the **gentle-bump instability**. It is enhanced if

- the number of particles in the bump is increased
- the bump becomes sharper (colder)
- the speed of the bump (V_0) increases, i.e., the situation approaches the cold two-stream case

The result that a monotonic function is stable is called **Gardner's theorem**. However, it does **not** imply that a non-monotonic distribution would automatically be unstable. If the bump is too gentle, the distribution may still be stable. The only way of finding this out is to calculate the imaginary

part of the frequency. A more powerful **stability** criterion than Gardner's theorem is provided by the **Nyquist method**. Considering the analytical properties of the function

$$G = \frac{1}{K(\omega,k)}\frac{dK(\omega,k)}{d\omega} \tag{7.72}$$

it is possible to show that the number of unstable electrostatic modes is

$$N = \frac{1}{2\pi i}\ln\frac{K(\infty)}{K(-\infty)}\,, \tag{7.73}$$

where $K(\pm\infty) = \lim K(\omega)$ when $\omega \to \pm\infty$. Gardner's theorem is a special case of this result.

Consider next a double-peaked distribution with a local minimum at speed u_0. For such a distribution the Nyquist method yields the **Penrose criterion**. It states that instability is **possible** if and only if

$$\int_{-\infty}^{\infty}\frac{F(u_0)-F(u)}{(u-u_0)^2}\,du < 0\,, \tag{7.74}$$

where $F(u)$ is a one-dimensional distribution function. The Penrose criterion implies:

- If there is a complete void of particles in the distribution function around u_0, the distribution is unstable.
- If a distribution is unstable according to the Penrose criterion, it is not possible to stabilize it by adding particles with velocity $u = u_0$ only. Almost the whole valley has to be filled.
- Penrose criterion applies to electrostatic modes only.
- A distribution function may have two maxima and still be stable.

7.3.3 Ion acoustic instability

In chapter 6 we found that the damping rate of the ion acoustic (IAC) wave depends on the ratio T_e/T_i. But what happens if the electron and ion distributions are in motion with respect to each other, thus making the total distribution function double-peaked (Figure 7.6).

Let the distribution functions be

$$F_{e0} = \sqrt{\frac{m_e}{2\pi k_B T_e}}\exp\left(-\frac{m_e(u-u_0)^2}{2k_BT_e}\right) \tag{7.75}$$

$$F_{i0} = \sqrt{\frac{m_i}{2\pi k_B T_i}}\exp\left(-\frac{m_i u^2}{2k_BT_i}\right)\,. \tag{7.76}$$

Using the Penrose criterion we can show that

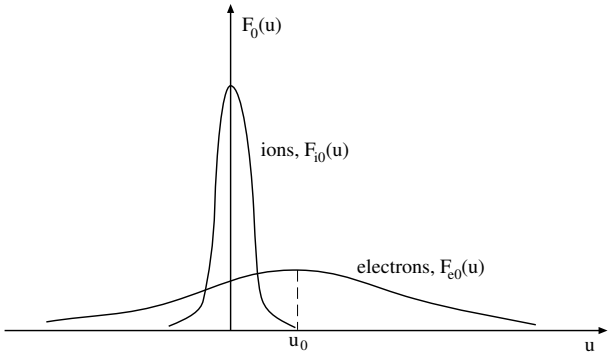

Figure 7.6: Maxwellian electron distribution streaming through a Maxwellian ion distribution with velocity u_0.

- for $T_i = T_e$ the plasma is stable if

$$u_0 < 1.3\sqrt{\frac{k_B T_e}{m_e}}\,, \tag{7.77}$$

- for $T_i \ll T_e$ the plasma is stable if

$$u_0 < \sqrt{\frac{k_B T_i}{m_i}}\,, \tag{7.78}$$

otherwise instability is possible. Note that in the cold ion case the stability limit is much smaller than in the case of $T_i = T_e$. This appears reasonable for the ion acoustic mode, but the Penrose criterion does not tell anything of the possibly unstable modes. To find the modes we must solve the dispersion equation.

It is reasonable (why?) to look for solutions in the range

$$\begin{aligned} \left|\frac{\omega_r}{k}\right| &\gg \sqrt{\frac{2k_B T_i}{m_i}} \\ \left|\frac{\omega_r}{k} - u_0\right| &\ll \sqrt{\frac{2k_B T_e}{m_e}}\,. \end{aligned}$$

A lengthy but straightforward calculation yields

$$\omega_r^2 = \frac{k^2 c_s^2}{1 + k^2\lambda_{De}^2} \quad ; \quad c_s = \sqrt{\frac{k_B T_e}{m_i}} \tag{7.79}$$

and

$$\begin{aligned} \omega_i \;=\; & -\frac{|\omega_r|\sqrt{\pi/8}}{(1 + k^2\lambda_{De}^2)^{3/2}} \;\times \\ & \left\{ \left(\frac{T_e}{T_i}\right)^{3/2} \exp\left(\frac{-T_e/T_i}{2(1 + k^2\lambda_{De}^2)}\right) + \sqrt{\frac{m_e}{m_i}} \left(1 - \frac{u_0}{c_s}\sqrt{1 + k^2\lambda_{De}^2}\right) \right\}. \end{aligned} \tag{7.80}$$

If $u_0 = 0$, this reduces to the IAC wave in chapter 6. When $T_e \gg T_i$, the instability condition can be found from the last term in (7.80). Close to the instability threshold the electron streaming and ion damping compete with each other. This also explains the fact that the positive slope of the distribution function alone is not sufficient for instability. It must be positive enough to win the damping by the background.

The ion acoustic instability requires relative drift of electrons and ions, i.e., net current. It thus is an example of **current-driven instabilities**. However, it is not sufficient to consider the net current alone to determine the stability of the system. In the formulas above both the temperature and the relative speed are critical parameters.

Ion acoustic wave is a fundamental mode in non-magnetized plasmas. In magnetized plasmas it becomes strongly damped perpendicular to the magnetic field. Even the damped mode is important as we will see in Chapter 9 when we will discuss the scattering of a radar signal from plasma. The conditions for the current-driven IAC instability can be met in a magnetized plasma if there is strong enough FAC.

7.3.4 Electrostatic ion cyclotron instability

Strong FACs can be found, e.g., above the auroral oval, where the ion-acoustig instability must, however, compete of the free-energy with other unstable wave modes, the most important of these being the the electrostatic ion cyclotron (EIC) wave (recall Fig. 6.4). Its dispersion equation can be derived from the general dispersion equation of the previous chapter. After a tedious calculation the real part of the frequency turns out to be

$$\omega_r \approx n\omega_{ci}\left[1 + \frac{T_e}{T_i}\Gamma_n(b_i)\right] \quad ; \quad n = 1, 2, ... \tag{7.81}$$

where $b_i = k_\perp^2 r_{Li}^2/2$, $\Gamma_n(b) = I_n(b)\exp(-b)$, and I_n is the modified Bessel function of the first kind.

When $T_e \approx T_i$, the solution for the marginally stable fundamental mode ($n = 1$) yields $\omega \approx 1.2\ \omega_{ci}$, $k_\parallel/k_\perp \approx 1/10$, and the critical speed is $u_{0c} \approx 13\ v_{thi}$. For higher harmonics the critical speed is larger. The EIC mode is particularly important when $T_e \approx T_i$, which makes the IAC mode strongly damped and the threshold for the EIC instability can be much smaller. However, once the IAC is destabilized it grows faster than the EIC mode.

7.3.5 Current driven instabilities perpendicular to B

The IAC and EIC instabilities are driven by FACs. Also the perpendicular currents lead to instabilities. The electrostatic approximation is good

in the low-β ionosphere. Both two-stream and Buneman instabilities arise from the kinetic theory. Actually, their rigorous treatment **requires** a microscopic discussion. An extra complication is due to the fact that these currents are often associated to spatial inhomogeneities, which makes the analytical treatment considerably more difficult. Usually heavy numerical computations with clever physical approximations are needed. The resulting instabilities are in many cases related to the lower-hybrid mode.

The perpendicular currents in the current sheets also drive instabilities related to electrostatic lower-hybrid modes. These instabilities have been considered e.g., as microscopic mechanisms of magnetic reconnection, where the current sheet disrupts. However, the relatively high beta makes the distinction between electrostatic and electromagnetic modes unclear. In fact, the lower-hybrid mode can be seen as the limiting case of the whistler mode for almost perpendicular propagation as the lower-hybrid mode can be found on the same dispersion surface in the $(\omega, \mathbf{k})$-space.

7.3.6 Loss-cone instabilities

Particle populations in a magnetic bottle have loss cone distributions. In such a distribution there is more energy in the perpendicular motion than in the parallel direction, which provides perpendicular free energy for instabilities. Perpendicular modes that may be excited are the electrostatic electron and ion cyclotron modes, or at short wavelengths the Bernstein modes. When the wave mode is excited the particles lose their excessive perpendicular energy and move to the loss cone from which they are lost through the end of the bottle. In this way, e.g., the magnetospheric bottle is leaky and particles precipitate into the upper atmosphere. This process of changing particles' pitch angles is often called **pitch-angle scattering** through wave-particle interaction. Another important pitch-angle scattering mechanism was met in Chapter 2 where we discussed non-conservation of the magnetic moment which also can lead to filling of the loss cone.

When a spacecraft with appropriate wave detector crosses the nightside equatorial region outside the plasmapause, it usually observes several harmonic bands of electrostatic electron cyclotron (Bernstein) modes. When these waves were found toward the end of 1960s, it was generally believed that they would explain the existence of the ever-present (but often subvisual) diffuse auroral precipitation. However, in mid-1980's it was found that these waves saturate at too low amplitudes to provide enough scattering to account for the nearly complete filling of the loss cone observed by low-altitude spacecraft above the auroral oval. As all alternative explanations have also failed, the question of wave-induced scattering has recently been revived and more refined analyses, including both the electron cyclotron and

whistler mode waves, are under way. This is an interesting example of the difficulties of space physics. After 40 years of research we still do not have a satisfactory explanation for such a common phenomenon as the diffuse auroral precipitation!

Loss-cone-driven electrostatic ion cyclotron modes have also been observed above the auroral oval. Again it should be stressed that the division between electrostatic and electromagnetic instabilities is a subtle issue. Loss cones can also drive electromagnetic modes. For example the diffuse ion precipitation in the dayside magnetosphere appears to be a result of electromagnetic ion cyclotron modes driven by anisotropies in the ion distribution.

7.4 Electromagnetic instabilities

There are more electromagnetic instabilities than electrostatic instabilities. Some of the macroscopic instabilities such as the firehose, mirror, kink, pinch, and helical instabilities are clearly electromagnetic because they involve a perturbation in the magnetic field. In this section we limit ourselves to some of the microscopic electromagnetic instabilities. Instead of trying to derive the dispersion equations we concentrate on the physical mechanisms behind the instabilities.

7.4.1 Anisotropy driven instabilities

In unmagnetized plasma the only electromagnetic mode is the O-mode. It can be driven unstable by an electron distribution which is strongly peaked (cold) in the direction of the wave propagation and thermal parallel to it. This may seem meaningless in space physics but this so-called **Weibel instability** has actually been applied in studies looking for the destabilization of current sheets.

The parallel propagating R- and L-modes are on the other hand very important in space physics because they can be in **cyclotron resonance** with the charged particles. As discussed in the previous chapter the Landau resonance is modified in a magnetized plasma into the form

$$k_{\parallel} v_{\parallel} = \omega - n\omega_{c\alpha} \,. \tag{7.82}$$

The case $n = 0$ is the Landau resonance. When $n = 1$ and $k_{\parallel} = 0$, we have a perfect resonance $\omega = \omega_{c\alpha}$ in the rest frame of the wave and a particle sees the wave all the time in the same phase. However, if there is a small difference between the frequencies, the particles experience an electric field which acts again to accelerate particles that are slightly slower than the phase velocity and to decelerate those that are slightly faster than the

phase velocity. Instability is possible if there are more fast particles than slow particles fulfilling the resonance condition. Now, however, a wider part of the phase phase is available than in the electrostatic case and an unstable distribution does not need to have a positive derivative, anisotropy can have the same effect. Of course, also a loss-cone distribution can fulfil the resonance condition to drive the R- and L-modes.

It is important to note that the perfect resonances of the R- and L-modes lead to wave damping. Consider an electron moving at perfect resonance close to the phase speed of the R-mode wave. If it is slower than the wave, it rotates in the same sense as the wave and sees the electric field which accelerates the particle to catch up with the wave. Thus the wave loses energy and is damped. However, if the electron moves faster than the wave, the wave seems to move backward in the electron frame and the electron sees the wave vector rotating in the opposite sense and there is no interaction between the wave and the particle. Thus at the resonance the flow of energy is always from the wave to the particles. This is one reason why the electromagnetic waves are very useful in plasma heating. The same reasoning applies to ions and the L-mode resonance.

However, below the electron cyclotron frequency the R-mode has the whistler branch that can be driven unstable by anisotropic distribution functions. Similarly there is an electromagnetic ion cyclotron instability below the ion cyclotron frequency. The ion cyclotron waves are important in magnetospheric plasma physics. Once generated they propagate as Alfvén waves over long distances. For example, ion cyclotron waves generated in the equatorial magnetosphere are known to propagate along the magnetic field down to the Earth where they are observable in form of magnetic pulsations. As they are generated in the region where the ion cyclotron frequency is of the order of 1 Hz, the pulsation periods span from about 1 s to longer periods.

Note that there are also much longer-period geomagnetic pulsations, up to several minutes. They are related to oscillations of the whole inner magnetosphere, e.g., as field-line resonances. One can imagine the dipole field lines as strings of a giant instrument that start to vibrate when disturbed by external forces.

The loss-cone distributions can under favorable conditions lead to emission of electromagnetic waves in X- and O-modes. A particularly important example is the **auroral kilometric radiation**. We will discuss it in Chapter 9 as an example of plasma radiation through cyclotron mechanism.

7.4.2 Ion beam instabilities

Finally, also ion beams can drive electromagnetic instabilities, both in the R-mode and in the L-mode. Figure 7.7 illustrates an ion distribution that,

when superposed with a hot background electron distribution, can be unstable for both modes.

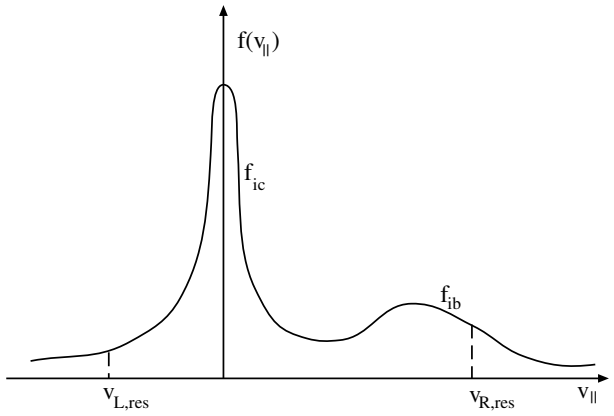

Figure 7.7: Ion beam resonances with R- and L-modes.

For the R-mode the resonance condition is

$$\omega = k_{\|} v_b - \omega_{ci} \tag{7.83}$$

and the excited mode is obviously the right-hand polarized component of an Alfvén wave, sometimes called **Alfvén whistler**. For increasing angle of propagation it goes over to the magnetosonic mode.

The excited L-mode is the mode approaching the electromagnetic ion cyclotron mode which at frequencies well below ω_{ci} is sometimes called **ion whistler**.

Finally, ion beams can drive non-resonant instabilities which propagate against the direction of the beam. The nonresonant mode is not a normal mode of a plasma but a purely growing perturbation resembling the firehose instability. These nonresonant modes are supposed to be important in the excitation of the observed turbulent fluctuations of the solar wind upstream of the bow shock.